SARS-CoV-2 epidemic after social and economic reopening in three US states reveals shifts in age structure and clinical characteristics

Nathan B Wikle[1,*], Thu Nguyen-Anh Tran[2,*], Bethany Gentilesco[3], Scott M Leighow[4], Emmy Albert[5], Emily R Strong[1], Karel Brinda[6,7], Haider Inam[4], Fuhan Yang[2], Sajid Hossain[8], Philip Chan[3], William P Hanage[6], Maria Messick[9], Justin R Pritchard[4], Ephraim Hanks[1], Maciej F Boni[2]

*equal contribution

[1]Center for Infectious Disease Dynamics, Department of Statistics, Pennsylvania State University, University Park, PA
[2]Center for Infectious Disease Dynamics, Department of Biology, Pennsylvania State University, University Park, PA
[3]Department of Medicine, Brown University, Providence, RI
[4]Center for Infectious Disease Dynamics, Department of Bioengineering, Pennsylvania State University, University Park, PA
[5]Department of Physics, Pennsylvania State University, University Park, PA
[6]Center for Communicable Disease Dynamic, Department of Epidemiology, Harvard T.H. Chan School of Public Health, Boston, MA
[7]Department of Biomedical Informatics, Harvard Medical School, Boston, MA
[8]Yale School of Medicine, Yale University, New Haven, CT
[9]Rhode Island Office of the Governor and Rhode Island Department of Health, Providence, RI

Correspondence: hanks@psu.edu, mfb9@psu.edu

Word Count: 6700

Date of this draft: Aug 13 2021

Abstract

In the United States, state-level re-openings in spring 2020 presented an opportunity for the resurgence of SARS-CoV-2 transmission. One important question during this time was whether human contact and mixing patterns could increase gradually without increasing viral transmission, the rationale being that new mixing patterns would likely be associated with improved distancing, masking, and hygiene practices. A second key question to follow during this time was whether clinical characteristics of the epidemic would improve after the initial surge of cases. Here, we analyze age-structured case, hospitalization, and death time series from three states – Rhode Island, Massachusetts, and Pennsylvania – that had successful re-openings in May 2020 without summer waves of infection. Using a Bayesian inference framework on eleven daily data streams and flexible daily population contact parameters, we show that population-average mixing rates dropped by >50% during the lockdown period in March/April, and that the correlation between overall population mobility and transmission-capable mixing was broken in May as these states partially re-opened. We estimate the reporting rates (fraction of symptomatic cases reporting to health system) at 96.3% (RI), 62.5% (MA), and 98.9% (PA). We show that elderly individuals were less able to reduce contacts during the lockdown period when compared to younger individuals, leading to the outbreak being concentrated in elderly congregate settings despite the lockdown. Attack rate estimates through August 31 2020 are 6.2% (95% CI: 5.7% – 6.8%) of the total population infected for Rhode Island, 6.7% (95% CI: 5.4% – 7.6%) in Massachusetts, and 2.7% (95% CI: 2.5% – 3.1%) in Pennsylvania, with some validation available through published seroprevalence studies. Infection fatality rates (IFR) estimates are higher in our analysis (>2%) than previously reported values, likely resulting from the epidemics in these three states affecting the most vulnerable sub-populations and the close matches between the states' reported COVID-19 deaths and excess deaths. Data in Pennsylvania may have been underreported for both non-hospitalized and hospitalized patients, casting substantial uncertainty on estimates of attack rate and infection fatality rate.

1 Introduction

The coronavirus SARS-CoV-2, the cause of coronavirus disease 2019 (COVID-19), has led to more than 600,000 deaths across the United States in just 18 months of transmission. During the initial wave in spring 2020, a critical question in managing the United States COVID-19 epidemic was whether regional re-openings of social and economic activity would result in rebounds of cases and hospitalizations [1]. Because population-level immunity to SARS-CoV-2 was still low at the time, the expectation was that increases in mobility and human contact would lead back to an upward trending epidemic curve during this time [2]. However, as hand hygiene, physical distancing, epidemiological awareness, and mask-wearing practices changed during spring 2020, increases in daily economic and social activity were not guaranteed to recreate the ideal transmission conditions of March. Additionally, no school session and the possible effects of drier/hotter weather [3] in summer were considered potential mitigators on viral transmission [4].

Despite these mitigating factors, epidemiological rebounds had begun in more than 40 states by July 1. Daily case numbers in the US – which had dropped from a peak of 30,000/day in early April to 20,000/day in late May – rebounded to 50,000/day the first week of July [5][6] driven by early re-opening policies in several large states. With a symptomatic case fatality rate (sCFR) rate in the 1% to 4% range [7–11] depending on epidemiological context and testing availability, more than a thousand of these daily new case numbers would result in death several weeks later. The absence of careful, gradual, managed reopenings during the May/June period were the likely cause of summer resurgence in parts of the southern US. It is of utmost public health importance that epidemic management and public health response continues to be approached with a strategic and adaptive plan that can utilize real-time epidemiological analysis (e.g. attack rate estimates, changing age/mobility patterns, clinical improvements) to contain and potentially reverse upward epidemic trends.

Here, we analyze the age-structured case, hospitalization, and death time series from three states – Rhode Island (RI), Massachusetts (MA), and Pennsylvania (PA) – that during summer 2020 did not experience substantial epidemic rebounds when compared to March/April levels. We evaluate eleven clinical data streams reported by the respective state health departments in a Bayesian inference framework built on an ordinary differential equations (ODE) age-structured epidemic model that includes compartments (clinical states) for hospitalization, critical care, and mechanical ventilation. We infer parameters on surveillance, transmission, and clinical characteristics of the first epidemic wave in RI, MA, and PA. We describe the patterns of persistently low transmission in these three states throughout August 31, compare these low-transmission scenarios to changes in human mobility metrics, and evaluate changes in age structure and clinical outcomes. We evaluate the impact of the spring epidemic on elderly populations in these three states, and we compare infection fatality rates (IFR) to published estimates from other parts

of the world. Preliminary analyses resulting from this work were regularly posted at https://mol.ax/covid and shared with the respective state departments of health. Statistical inference described here — on attack rates, underreporting, changing age-profiles — can guide more granular real-time decision making and public health messaging than direct data streams.

2 Results

2.1 Epidemic characteristics during and after lockdown

In Rhode Island, Massachusetts, and Pennsylvania, from early March to early April, we inferred a reduction in the composite transmission parameter β_t describing person-to-person contact (mixing) rates and the probability of virus transmission per unit contact. From the March 5-15 period to April 1, population mixing rates dropped by 65.2% (95% CI: 51.4% - 78.2%) in RI, by 79.8% (95% CI: 61.5% - 87.0%) in MA, and by 95.4% (95% CI: 92.8% - 97.4%) in PA (Figure 1). During this period, contact rates were dropping through stay-at-home orders, bans on large gatherings, and business/school-closures at the same time as improved hygiene behaviors were being increasingly adopted; thus, it is not possible to determine the individual contributions to β_t of mixing reduction and hygiene improvement. The reductions seen in β_t in March and early April are reductions in *transmission-capable mixing* that result both from fewer person-to-person contacts and lower infection risk per contact. These reductions in mixing may seem very large, but note that in a heterogeneously exposed population, mixing rates for large highly connected groups can drop by large amounts with only a modest drop in the population's effective reproduction number R_t if a smaller sub-population maintains a chain of infection due to an inability to completely zero-out contacts. For example, if 90,000 office employees can work from home and contact only their families but 10,000 elderly care home residents still require contact with medical and care staff, then a full business shutdown may result in a 90% reduction in mixing patterns but a measured or apparent $R_t \approx 1$ if a stable chain of infection is maintained in nursing homes and elderly care residences. Our estimated reductions in transmission-capable mixing are consistent with published estimates of changes in R_t and mobility [12–16].

Changes in the inferred population-mixing component β_t can be compared to mobility metrics [17,18] based on location-enabled smartphone data trails, which allow calculation of time spent at home versus outside the home. Two independent mobility data sources, Facebook and SafeGraph [19,20], provided daily estimates for the fraction of tracked users leaving home at least once in a 24-hour period. Despite values varying slightly across states and significantly between user bases, all mobility data examined have a common shape and timing: an initial baseline in early March (84%-86% of users leaving home for Facebook; 75%-77% for SafeGraph), and a subsequent dramatic decrease from 3/15 to 3/31 (64%-

67%; 52%-55%). This low fraction of users leaving home (at a minimum, once daily) is maintained until about April 20, followed by a slow increase to a slightly more cautious 'new normal' (77%-81%; 66%-69%) through July and August (Figure 1). A resumption of population mobility in early May suggests that improvements in hygiene, personal distancing, mask wearing, selective travel, and/or smaller event sizes were likely factors keeping $R_t < 1$ and new case numbers declining.

Not all symptomatic SARS-CoV-2 infections are reported to state-level health systems. As it is difficult to make distinctions among asymptomatic, sub-clinical, mildly symptomatic, and symptomatic infections, here we call an infection *symptomatic* if the symptoms are pronounced enough that a person with convenient zero-cost access to health care would choose to visit a hospital or clinic. Using the delays between time series of cases, hospitalizations, and deaths, we can estimate the fraction ρ of symptomatic cases that are reported to the health system [21,22]. We do this without making assumptions about the case fatality rate or infection fatality rate. Complications present themselves as underreporting in the hospitalization data sets is common; see discussions in Supplementary Sections 1.3, 1.4. One clear example of this difficulty is when only current hospitalizations are available (MA and PA), a good model fit requires that the duration of hospitalization is known or identifiable; this is complicated by the fact that hospital stays come in several categories (admission to ICU, requiring mechanical ventilation) and can be censored by death events. In Massachusetts and Pennsylvania, there is not enough information in the remaining data streams to confidently identify the duration of hospitalization (Figure 5B). Age-stratified probability of hospital admission in MA and PA is constrained to be close to estimated values obtained from Rhode Island data (Figure 5E). Our estimate for the reporting rate ρ in Massachusetts is 62.5% (95% CI: 54.5% - 78.5%). Rhode Island has complete reporting of hospitalization incidence, made possible by the state's small size and a reporting system covering several small hospital networks that include all hospitals in the state. We estimate that 96.3% (95% HPD: 87.1% - 99.8%) of symptomatic COVID-19 cases are reported to RIDOH (after May 2020). RIDOH staff and affiliated physicians reported that patients were being turned away in early March due to lack of tests, and March reporting rates are estimated at less than 30% (March 15 estimate is 18.1%, 95% CI: 9.9% - 33.1%); see Figure 5A. For PA, our estimate of the symptomatic case reporting parameter ρ is 98.9% (95% CI: 94.5% - 99.9%), and this high rate may be the result of underreporting in multiple data streams; see *Discussion*.

Reporting rate estimates combined with age-specific estimates of asymptomatic infection [24] allow cumulative attack rates to be estimated (Figure 3). The probability of asymptomatic infection is difficult to estimate for SARS-CoV-2 as this requires prospective follow-up in either a household or cohort design, with few studies including enough age groups for between-age comparisons [25–28]. We use published estimates from Davies et al [24], as the age-based asymptomatic fraction data from individual studies has too much variation to provide meaningful estimates (Figure S1). The August 31 population

attack rates for SARS-CoV-2 are 6.2% in Rhode Island (95% CI: 5.7% - 6.9%), 6.7% in Massachusetts (95% CI: 5.4% - 7.6%), and 2.7% in Pennsylvania (95% CI: 2.5% - 3.1%); see Figure 3. These attack rate estimates use symptomatic case data through September 6, as an infection on August 31 would have its mean time of symptoms occurrence six days later. Note that only 1% of Pennsylvanians had reported as symptomatic and confirmed COVID-positive through September 6 2020, and this may be an undercount.

Our Rhode Island attack rate is able to be validated with a 2.2% late-April attack-rate estimate obtained from a household sero-survey [29] and 0.6% early-April estimate from blood donors [30] (population biased towards healthier individuals). Our Pennsylvania-wide attack rate has a Philadelphia early-April estimate of 3.2% as a comparator [31], as well as a 6.4% estimate from July using serum from dialysis patients (not adjusted for race or socio-economic indicators, and thus biased upward) [32]. The unadjusted dialysis-patient seroprevalence in Massachusetts was estimated 11.3% in July 2020 [32], about twice our estimate. Attack rate estimates continued to be reported to state-level DOHs through mid-March 2021 (see http://mol.ax/covid), in general agreement with studies being released during this time (see *Discussion*).

Estimates of reporting rates allow for age-specific fatality rate estimation in all three states (Table 1). First, these results show that the age-adjusted infection fatality rate (IFR) for all three states is higher than the typically quoted 0.5%–1.0% range over the past eight months of IFR-estimation [33–37], but note that epidemics that infect the most vulnerable segments of a population first may be associated with higher-than-average IFRs (see *Discussion* and [36,38]). Population-weighted IFR estimates are 2.5% (95% CI: 2.0% – 2.8%) for the Rhode Island epidemic during March-May, 2.1% (95% CI: 1.7% – 2.5%) for the Massachusetts epidemic during March and April, and 2.8% (2.7% – 3.1%) for the Pennsylvania epidemic from March through June. These estimates are presented for the early stage of each state's epidemic as our inference suggests that mortality rates dropped from spring 2020 to summer 2020 (section 2.2), consistent with observations in New York City showing a higher than normal IFR during the first three months of the epidemic in 2020 [38]. It is well known that the IFR depends strongly on age, gender, co-morbidities, socio-economic factors, and race [39][40]. Our estimated age-stratified IFRs indicate that fatality rates are highest (>3%) in the 60+ age groups, still very high in the 40-59 age group (estimates ranging from 0.3% to 1.2%), and lower in the <40 age group (<0.1%). The age-adjusted symptomatic case fatality rate (sCFR) is estimated to be 3.8% (RI), 3.2% (MA), and 4.4% (PA). The hospitalization fatality rate (HFR) shows the least variation by age, with fatality rates >9% for the >40 age groups, a lower 3.3% to 4.8% HFR for 20-39 age group, and no estimates possible for individuals under 20.

2.2 Changes in age-stratified contact patterns and clinical outcomes during the epidemic

We investigated changing age-specific contact rates during the three state epidemics, based on observed changes in age distribution and well-documented reporting of outbreaks in nursing homes. In 2020, age-contact matrices began to be measured for the COVID-19 socially-distanced era [41–45], and we thus allow for two mixing patterns in our population – one mixing pattern during the spring 2020 lockdown and a second pattern in late spring and summer after the lockdowns were lifted. We infer eight relative mixing levels for each age class (relative to the 0-9 age group) and use a symmetric parametrization where contact rates are described per age-group pair (i.e. $c_{ab} = c_a \times c_b$) where c_a is the mixing rate for age group *a;* see equations (S6). Use of the Belgian CoMix study's contact rates was evaluated [46,47], but these more highly parameterized matrices did not provide a better fit for our six-month time series (ΔDIC > 70 for all three states). Age characteristics of each state epidemic are shown in Figure 4 (*top rows*)**,** and the inferred contact parameters are shown in Figure 4 (*bottom rows*); inference of contact rates is influenced by the model assumption that the 0-19 age group is 60% as susceptible to infection as the other age groups [24]. In all three states, the lowest inferred contact rates during lockdown were for the 0-9 and 60-79 age groups, reflecting closed schools and possibly the caution with which older individuals approached their risk of infection. However, the relative contact rates for individuals in the ≥80 age group were much higher: 2.6 (95% CI: 2.4–2.9) in RI, 6.1 (95% CI: 4.9–7.0) in MA, and 4.8 (95% CI: 4.5–5.1) in PA. This suggests that social distancing and lockdown were more difficult for individuals that needed additional care or lived in congregate care facilities. The shift from an older age profile to a younger age profile is apparent in all three states' epidemics as the epidemics progressed from spring to summer (Figure 4, *top rows*).

Improvements in clinical management of hospitalized COVID-19 cases, due to the use of prone positioning [48,49] or more frequent use of corticosteroids [50,51], may have led to lower mortality relative to epidemic size during the more recent (June-Aug) stages of the epidemic when compared to March-May mortality rates [52–54]. To estimate the effects of some of these interventions, we assess whether progression from hospitalization to critical care changed between the early stages and the later stages of the epidemic. Our model uses the relative age proportions described by Lewnard et al [23] who estimated probabilities of progression from medical-floor care to critical care to be between from 30% to 50% (comparable to other estimates [55,56]) for all nine age bands used in this study. These age-specific probabilities are scaled in our model (keeping the relative age probabilities the same), independently for each state, as patterns of hospital admission and clinical algorithms for ICU admission are likely to differ somewhat between health systems and hospitals; the scaling parameter is estimated. In Rhode Island, the age-adjusted probability (posterior median) of ICU admission for a hospitalized case dropped from 26.0% (95% CI: 20.4%–31.0%) to 16.5% (95% CI: 11.6%–21.0%) with an inferred breakpoint at May 26 2020

(95% CI: May 6 – June 2). In Pennsylvania, the age-adjusted ICU admission probability dropped from 39.5% (95% CI: 36.7% – 43.1%) to 28.0% (95% CI: 24.4%–33.8%), with an inferred breakpoint of June 19 (95% CI: June 13 – June 22). In Massachusetts, this probability dropped from 29.2% (95% CI: 23.9% – 36.3%) to 21.2% (95% CI: 17.5% – 29.0%), with the likely change occurring between late-April and mid-June (Figure 5D).

A second approach to confirming trends on improved clinical case management would be to look directly at changes in mortality. However, the complexity in this analysis lies in the different possible clinical paths that lead to a fatal outcome. In most states, reported mortality trends combine deaths occurring in hospitals with deaths occurring at home (i.e. in congregate care facilities); these data streams are separated in RI/PA but not MA. Our model allows for inference of at-home mortality, with the at-home symptomatic case fatality ratio estimated at between 20% to 35% for the ≥80 group, and 5% to 20% for the 70-79 age group (Figure 5C). This allows us to separate mortality trends into home and hospital, but hospital mortality alone is still a complex composite of probability of death on the medical-floor level of care and probability of death in the ICU (with and without ventilation). For this reason, we chose ICU admission as the clinical progression marker where we could evaluate a simple trend of improved case management. Estimated at-home mortality may be affected by the choice of using reported death counts or excess death counts [57] in an analysis, and using excess deaths in our inference did result in slightly higher estimates of at-home mortality for the >70 age groups (Supplementary Material, section 7).

Model selection analyses showed that a model with changing age-mixing patterns and improved clinical management was a better fit than models without these features (ΔDIC > 27 for all three states; Table 2).

3 Discussion

This is among the first studies to evaluate multiple simultaneous clinical data streams with an epidemic transmission model. The analysis of concurrent data streams is necessary to describe certain important but unreported characteristics of regional SARS-CoV-2 epidemics; these include underreporting of cases, changing age patterns of infection, changing patterns of clinical progression, and an understanding of mortality rates outside hospital settings. The inclusion of multiple age-structured data streams on death and hospitalization allows for statistical estimation of symptomatic case underreporting — a quantity that is generally resistant to robust estimation especially in public-health reporting systems that (1) mix active and passive surveillance, (2) mix multiple diagnostic tests and testing visits, and (3) have not made estimates of their catchment areas. With an estimate of symptomatic case underreporting (here, via ρ), we can estimate the population-level SARS-CoV-2 attack rate in each state by summing the reported symptomatics, the

unreported symptomatics, and an externally estimated number of asymptomatics. One month later, an attack rate estimate can be validated by comparing to results from a seroprevalence survey. Four seroprevalence estimates available for RI, MA, and PA show no major inconsistencies with our results. It is important to remember that SARS-CoV-2 sero-surveys can be subject to biases depending on approaches to recruitment (which can overestimate seropositivity if enriched for individuals who are more likely to have been infected, e.g. individuals who consent because of past symptoms), the time since the original infection (antibody titers wane over time), and the specific test used [58].

Our results indicate that in autumn 2020 Rhode Island, Massachusetts, and Pennsylvania were nearly fully susceptible to a winter epidemic wave of SARS-CoV-2. Continual attack-rate estimation will be crucial through 2021 to identify pockets of uninfected and unvaccinated individuals. Specifically, real-time age-specific attack rate estimation is important for vaccination planning, as age groups experiencing the least infection may need to be prioritized during both initial and annual vaccination campaigns.

Similar to attack-rate estimation, mobility tracking can give us a partial window into the effect that distancing policies or lockdowns are likely to have on viral transmission. In May 2020, the positive correlation between stay-at-home metrics and viral transmission vanished in all three states (as in [59]), resulting in a summer with population mixing levels at nearly pre-pandemic levels (i.e. people not staying at home) but viral transmission close to its post-lockdown low point. It is reasonable to suggest that at least some of this is explained by (1) weather increasing the proportion of contacts made outdoors, where transmission is known to be much less likely, and (2) a shift from mixing outside the home to inside the home, i.e. less time spent at work and more time with family. It is not straightforward to relate measures of population movement to opportunities for transmission, for many reasons including the collinearity of mixing with many other factors that can influence it. Essentially, rather than absolute measures of mixing, the blue lines in Figure 1 can be interpreted as levels of population mixing that are capable of producing transmission ("transmission-capable mixing"). By cancelling large events, promoting stringent hygiene measures, requiring masking, closing schools, restricting gathering sizes, and creating new guidelines for business operations, the epidemics in RI, MA, and PA were contained during the summer months while allowing the states' residents to continue most essential activities including small/medium outdoor events. In summer 2020, aggregate measures of population movement were at or near normal levels but mixing leading to transmission was substantially reduced.

It is useful to compare our results on attack rate and contact patterns with those obtained through different methodological approaches. Our US state-level inference was performed on a data stream of cases, hospitalizations, and deaths, with an externally estimated asymptomatic fraction; we estimated mixing/mobility levels, underreporting for symptomatics, and the infection fatality rate. The state-level analyses presented by Unwin et al [60] and Monod et al [61] performed inference on a data stream of cases,

mobility, and deaths, with an externally estimated IFR; they estimated age-pair contact rates and underreporting for infections. Certainly, both approaches' results are sensitive to the external estimates used. The combined effect of underreporting and asymptomatic infection (Unwin's infection ascertainment ratio, IAR, defined as the number of reported cases divided by the total number of infections) has similar estimates whether using our approach or Unwin's — 0.58 (here) and 0.51 (Unwin) in Rhode Island, 0.43 and 0.38 in Massachusetts, and 0.59 and 0.51 in Pennsylvania. However, the June 1 2020 attack rates estimated with these two approaches differ by a factors of two or three — 4.1% (here) and 7.5% (Unwin) in RI, 5.0% and 11.2% in MA, and 1.5% and 4.4% in PA — suggesting that the external estimates of IFR and the asymptomatic fraction play a large role in attack rate estimation. Comparing our attack-rate estimates to those of Monod (through late Oct 2020), we see estimates of 10.9% (our method [62]) and 11.0% (Monod [61]) in RI, 8.2% and 13.0% in MA, and 6.8% and 6.6% in PA. For MA and RI, these late-October estimates are not consistent with CDC's commercial laboratory seroprevalence survey [63] (about 5% in RI, 4% in MA, and 7% in PA), or the CDC blood-donor survey [64] seroprevalence estimates (4% in RI, 5% in eastern MA, and 5% in central/southwestern PA). The CDC results need to be evaluated in the context of rising and waning seroprevalence, which may result from a high assay threshold and/or not accounting for antibody waning in seroprevalence estimates [65,66].

Our data and inference support a changing contact pattern in May/June 2020, with much higher mixing levels for the 10-29 age group in summer than in spring. This contact pattern was not explicitly tested by Monod et al, although they did find that the 20-49 age group was the primary driver, at a national scale, of transmission in summer and fall 2020; the influence of the 20-49 age group on transmission appears to be small in RI, MA, and PA as these states did not have rebound epidemics in summer 2020. Despite differing approaches as to which quantities are treated as data and which ones are estimated, our study and Monod's do share a point of consistency in the importance of the 20-29 age group to maintaining transmission in summer 2020.

In our analysis, infection fatality rates are estimated to be higher than in recently summarized analyses [33–37], and the differences are particularly notable in the 50-79 age group where we infer IFRs that are 1.5 to 2.5 times higher than previous estimates. Our IFR estimates for the 20-49 age groups are most similar to those presented by Brazeau et al [37]. And the all-ages IFRs in MA and RI are as high as some of the highest estimates [9] of the Levin et al [67] study. These high estimates may correspond to a high degree of exposure heterogeneity in the studied epidemics. As it is known that RI and MA had substantial outbreaks in elderly care facilities in the spring, it is likely that this focused epidemic passed through a more susceptible sub-population (individuals who cannot fully quarantine or distance due to needing routine care) that is also more likely to progress to severe clinical outcomes including death. This was observed in New York City, where an infections-weighted IFR of 1.39% was estimated for the first

several months of the epidemic in 2020. When weighting our estimates by the number of infections in each age class (this is a particular epidemic's IFR as opposed to the IFR for a randomly selected person in the population), we obtain IFRs of 2.24% for RI and 1.53% for MA.

A second possible explanation for the high estimates of IFR and sCFR presented here is that RI, MA, and PA reported COVID-19 death counts similar to excess death counts for the same period. This implies that in locations where deaths were undercounted, the excess death counts are closer to the true COVID-19 death counts. A third possibility (for Pennsylvania only) that would influence both IFR and attack-rate estimates is that both case and hospitalization data were underreported. A 1% symptomatic attack rate in PA over the first six months of the pandemic is lower than expected, but the underreporting fraction estimate (ρ = 98.9%) in our analysis is likely wrong if hospitalization numbers were also underreported. The reporting rate ρ determines the attack-rate estimates; if ρ is overestimated the infection fatality rates presented here would also be overestimated. This may be the reason that our estimated fatality rates for PA appear to be unreasonably high, and that the PA attack-rate estimate through August 31 2020 is so low.

The symptomatic case fatality ratios (sCFR) inferred for RI, PA, and MA (estimates range from 3.2% and 4.4%) are in the higher ranges of previously reported estimates [8–11,68–70], suggesting that the individuals infected during the spring wave and summer lull were more likely to progress to symptoms than the average person in the population. Again, this is consistent with the observation that children were the least exposed in the spring and summer months, and thus the exposed population was both more likely to progress to reportable symptoms and more likely to progress to severe clinical outcomes.

In late 2020, an unfortunate diversion in policy discussion was the consideration of an epidemic management approach that would encourage younger/healthier populations to become infected [71]. Our state-level analyses indicate that older individuals are not able to fully isolate during lockdown periods. This makes a 'protecting the vulnerable' strategy unworkable, as vulnerable individuals will still require essential care and contact with other humans. Any policy aiming to protect vulnerable individuals while allowing the remainder of the population to mix and move freely would almost certainly fail at preventing viral introduction from the general population into vulnerable populations. In our analysis, during the March/April lockdown period, the ≥80 contact rate was the highest or among the highest when comparing across age groups (Figure 4). As individuals in the oldest age groups are relatively unaffected by lockdown, the best way to protect these (and other) vulnerable populations is to limit the spread in the general population.

3.1 Limitations and Recommendations

One key limitation in using data streams rooted in symptomatic case reporting is the inability to infer asymptomatic infection rates. These rates must be estimated independently from cohort follow-up or contact tracing. They are susceptible to bias in the younger age groups if children test negative due to low viral loads and are classified as negative rather than asymptomatic. Studies are also susceptible to design errors when the protocol or data collection does not allow for differentiation between pre-symptomatic and asymptomatic individuals (Supplementary Materials, Section 1.8). Although the majority of studies have converged on an age-adjusted "60% symptomatic" number, age-specific estimates come with less certainty and differences in diagnostic tests and testing protocols have resulted in substantial variation in these estimates (Supplementary Materials, Figure S1).

The data streams we present here do not allow us to evaluate the degree to which the epidemic runs through specific sub-populations (e.g. congregate care settings, college students) that are more vulnerable, susceptible, or transmit more easily. To measure variability in transmission and susceptibility from state-level data, we suggest including these common data types into the same databases/datasheets currently maintained by all state DOHs as part of routine COVID reporting: (1) contact counts and positivity rates from contact tracing efforts, (2) positive/negative case counts and inclusion criteria from asymptomatic random screening programs [72], and (3) a datasheet keyed on a categorical variable of 'infection source event' with confirmed patient counts, ages, and dates of reporting listed [73,74]. Among these data types, the asymptomatic screening efforts are likely the easiest to turn into a standardized daily data stream as samples taken from screening programs pass through the same sample/data processing pipelines as samples from symptomatic patients. These data would also allow for real-time tracking of prevalence.

We cannot exclude the possibility that our reporting rate estimate (ρ) is incorrectly estimated due to model misspecification or data integrity problems. In addition symptomatic reporting is likely to vary by age [38] and by availability of testing, making a single ρ-estimate a coarse descriptor of individuals' reporting tendencies. This is the reason that validation with seroprevalence estimates is crucial for estimating underreporting in public health surveillance systems. The entire inferential framework for ρ assumes that hospitalization data are complete, that death data are complete, and that various measures of hospitalization duration have been independently estimated or are identifiable from our data. The biggest leap in these assumptions comes in the completeness of hospitalization data, as both Massachusetts and Pennsylvania have relied on hospitalization data streams that are partially complete. This is a reminder — during the pursuit of rapid results with pre-packaged epidemiological tools and dashboards — to carry out the somewhat slower due diligence of understanding the sampling frames of all data streams included in an

analysis. If hospitalization numbers are underreported in other states as well, national-level analyses of hospitalization numbers would need to acknowledge and account for this.

Finally, we were not able to use any published contact matrices for the lockdown period as these data did not exist for our populations at the time our work was being done [41–45]. Thus, we used nine independent mixing rates for the nine age-classes in our model (and assumed that contact between two age groups is proportional to their two mixing rates); the data are unlikely to have enough resolution to infer 81 independent mixing parameters.

Through 2019, infectious disease epidemiology was neglected in the United States for more than half a century because of our status as a developed country, with a secure food supply, a sanitary water system, few persistent disease vectors, high public hygiene standards, and ample supply of therapeutics and vaccines. We were not prepared in 1981 when the HIV epidemic was uncovered, and with no leadership from the federal government in 2020, we were underprepared at state level for the SARS-CoV-2 epidemic as few individuals remained with knowledge from the early struggle against HIV. Specifically, the right data systems were not in place at state level DOHs to provide consistent and interpretable data streams allowing epidemiologists to make real-time assessments on epidemic progression and success of control efforts. State-level systems in the US require more funding from the federal government or centrally designed (and funded) reporting tools from the Centers from Disease Control and Prevention that would allow all states to consistently report the same high-quality data types. The rationale for this systems upgrade would be to advance our surveillance systems to those of countries like New Zealand, Hong Kong, Singapore, Vietnam, Taiwan, and South Korea that successfully controlled epidemic waves and introductions of SARS-CoV-2.

4 Methods

4.1 Case Data

Eleven data streams were assembled from three state department of health websites and data dashboards: (1) cumulative confirmed cases, (2) cumulative confirmed cases by age, (3) cumulative hospitalized cases, (4) cumulative hospitalized cases by age, (5) number of patients currently hospitalized, (6) number of patients in ICU currently, (7) number of patients on mechanical ventilation currently, (8) cumulative deaths, (9) cumulative deaths by age, (10) cumulative hospital deaths, (11) cumulative hospital discharges, with streams 6 and 11 missing in PA, and 10 and 11 missing in MA. Cumulative hospitalizations (data streams 3 and 4) in MA and PA were reported as a subset of symptomatic cases (via follow-up case investigations) and were excluded from the analysis. Reporting started on Feb 27 (RI), Mar 1 (MA), and

Mar 6 (PA), and data sets used in this analysis comprise about 180 days of data through September 6. Age-specific counts often summed up to be less than the corresponding total daily counts of new symptomatic cases, new hospitalizations, or new deaths. This was common due to lack of age reporting in some proportion of cases. We assumed missing age-structured data to be missing completely at random when their sum was less than the total count. Data from random asymptomatic screening efforts (elderly care facilities, health care workers) were available for five months in RI and one month in MA. RI screening data were incorporated into the analysis to adjust the inference on the reporting fraction (ρ), as these individuals did not report to the health system but were sought out by the health system.

4.2 Mobility Data

The first set of mobility data is provided by the COVID-19 Mobility Network [19] and is derived from users of the Facebook mobile app with the location history option enabled, representing approximately 0.8% of MA, 1.1% of PA and 1.1% of RI. Each user's location is binned into tiles, approximately 470m × 610m at Pennsylvania's latitude. These are aggregated by home county and date, and reported as the fraction of users who remain in one tile for the whole day. In this paper, we report state-level data by weighting these proportions by each county's population, per the U.S. Census' 2019 estimates. These estimates are not adjusted for the demographics of Facebook's user base.

The second set of mobility data is provided by social distancing metrics recorded by SafeGraph [75]. The data were derived from GPS pings of anonymous mobile devices. A common nighttime location for each device over a 6-week period was defined to be the device's "home" and daily GPS pings were analyzed to determine whether the device exhibited certain behaviors including completely staying at home, working part time, working full time, etc. The counts were aggregated at the Census Block Group (CBG) level, which is the second-smallest geographical unit for which the US Census Bureau publishes data. A state-level percent at home fraction can be calculated by dividing the 'completely at home' devices in a state by the total devices in that state, however one step was taken prior to this calculation as outlined in the data analysis methodology for the Stay-At-Home Index provided by SafeGraph [76]. The step included was a correction for sampling bias at the CBG level by resampling with a stratified reweighting method described in the supplementary materials [77] (see Supplementary Materials Section 1.6.2).

4.3 Mathematical Model

A standard age-structured ordinary differential equations (ODE) model was used to describe the dynamics of SARS-CoV-2 spread in a single well-mixed population. The model includes 30 compartments for different clinical states including susceptible, exposed, asymptomatic, infected, hospitalized, in ICU, on

mechanical ventilation. Multiple consecutive compartments are used for most clinical states to reduce the variance on length-of-stay in various stages in disease progression. Model diagram shown as Figure S2 and equations shown in the Supplementary Materials Section 2.

Model parameters fall into several categories including parameters on contact rates, lengths of stay in various clinical states, and probabilities of progression from one state to another. Daily community-level transmission-capable mixing rates β_t were inferred from the data, while age-specific contact rates for hospitalized individuals had to be fixed as too little data exist on these parameters. Asymptomatic individuals are assumed to be half as infectious as symptomatic individuals (similar to other models' assumptions [78,79]).

Lengths of stay and age-specific probabilities of clinical progression were available from numerous data sets documenting COVID-19 hospitalized populations; details in Supplementary Materials Section 2, Table S1 and https://github.com/bonilab/public-covid19model. When clinical parameters were inferred, their median estimates were typically close to observed values in hospital or surveillance datasets. No data were available in RI, MA, or PA to infer the asymptomatic fraction for each age group, and these were obtained from cohort analyses available at the time (see Supplementary Materials Section 1.8) and the inferred age-specific asymptomatic fractions in Davies et al [24]; the Davies fractions were used for the final model runs.

4.4 Statistical Inference

Given the various – and at times incomplete – data sources available for each state, we chose a flexible Poisson-Gamma process-based likelihood framework to facilitate inference of ODE model parameters while accounting for model uncertainty. In particular, the cumulative cases, hospitalizations, deaths, and hospital discharge data were assumed to be realizations of conditionally independent, inhomogeneous negative binomial processes, with time-varying process rates defined by the expected deterministic ODE output. The likelihood function for each age-structured data stream is then a product of independent, negative binomial increments, with means determined by the corresponding age-structured component of the ODE system over each increment. Means for observed new symptomatic cases were equal to ODE system predictions multiplied by a symptomatic reporting rate constant, and means for observed new hospitalized individuals were equal to ODE system predictions. The time from symptoms to presentation was fixed at 2.0 days (see Supplementary Section 5.2). When random screening data are available, we adjust the mean of the number of new symptomatics to include an additional additive term equal to the rate of random testing times the probability of a positive test. Dependence across data streams is assumed to be captured by the ODE system. Total data streams, summed over all age classes, were viewed as the sum of independent negative binomial random variables, and are as such negative binomial random

variables themselves, with mean given by the sum of the age-specific means. When both age-structured and total data are available, we assume any missing age-structured data are missing completely at random, and approximate the joint likelihood of the total and age-structured counts by ignoring overdispersion and assuming that, conditioned on the total data, the age-structured counts are multinomially-distributed with probabilities proportional to the age-structured ODE means. Data on current hospitalizations, as well as current numbers in intensive care units, and current intubated individuals were modeled using reported weekly totals. The total number of intubated individuals, individuals in intensive care units (but not intubated) and hospitalized individuals (not in intensive care units) were each modeled as independent Gaussian random variables with means equal to the corresponding totals predicted by the ODE system, and with unknown variances. Additional details on the likelihood framework can be found in Supplementary Materials, Section 3.

We chose a Bayesian approach to inference, allowing for appropriate penalization of time-varying parameters and a combination of strongly and weakly informative priors for parameters relating to clinical progression of disease. The composite rate parameter, β_t, describing person-to-person contact mixing, is constructed via a cubic B-spline, with a random walk prior (penalized regression spline with 1st order differences) on the B-spline coefficients to penalize overfitting. In RI and PA, the symptomatic reporting rate ρ is constructed as an I-spline with a similar prior; in MA it is assumed to be constant across time. Additional parameters found within the ODE system, including length of hospital stay and proportion of cases needing hospitalization within each age class are given uniform priors with bounds determined by expert judgement, while negative binomial dispersion parameters are given weakly informative exponential priors and Gaussian variance parameters are given conjugate inverse-gamma priors. Given these priors and the previously defined likelihood, we constructed a Markov chain Monte Carlo (MCMC) algorithm to sample from the posterior distribution of model parameters. Block updates for parameters were obtained using a random walk Metropolis-Hastings algorithm with an adaptive proposal distribution [80]. For each state, five independent chains were run for 300,000 iterations, with the first 100,000 samples discarded as burn-in. Convergence was assessed qualitatively across the five chains. R and C++ Code is posted at https://github.com/bonilab/public-covid19model.

Funding

MFB, TNAT are funded by a grant from the Bill and Melinda Gates Foundation (INV-005517). FY is supported by the NIH/NIAID Center of Excellence in Influenza Research and Surveillance contract HHS N272201400007C. KB was partially supported by the National Institute of General Medical Sciences of the National Institutes of Health under award number R35GM133700. WPH is funded by an award from

the NIGMS (U54 GM088558). JA is funded by the Penn State MRSEC, Center for Nanoscale Science, NSF DMR-1420620. EH was partially supported by NSF DMS-2015273. Thanks to Larry Madoff and Catherine Brown at the Massachusetts Department of Public Health for help in interpretation of the MassDPH online data sources.

References

1. Fineberg HV. Ten Weeks to Crush the Curve. N Engl J Med. 2020;382: e37. doi:10.1056/NEJMe2007263

2. Baker RE, Yang W, Vecchi GA, Metcalf CJE, Grenfell BT. Susceptible supply limits the role of climate in the early SARS-CoV-2 pandemic. Science. 2020;369: 315–319. doi:10.1126/science.abc2535

3. Morris DH, Yinda KC, Gamble A, Rossine FW, Huang Q, Bushmaker T, et al. The effect of temperature and humidity on the stability of SARS-CoV-2 and other enveloped viruses. bioRxiv. 2020; 2020.10.16.341883. doi:10.1101/2020.10.16.341883

4. Carlson CJ, Gomez ACR, Bansal S, Ryan SJ. Misconceptions about weather and seasonality must not misguide COVID-19 response. Nat Commun. 2020;11: 4312. doi:10.1038/s41467-020-18150-z

5. Times TNY. Covid in the U.S.: Latest Map and Case Count. The New York Times. 20 Jul 2020. Available: https://www.nytimes.com/interactive/2020/us/coronavirus-us-cases.html. Accessed 22 Oct 2020.

6. Johns Hopkins Coronavirus Resource Center. [cited 22 Oct 2020]. Available: https://coronavirus.jhu.edu/MAP.HTML

7. Ahammed T, Anjum A, Rahman MM, Haider N, Kock R, Uddin MJ. Estimation of novel coronavirus (covid-19) reproduction number and case fatality rate: a systematic review and meta-analysis | medRxiv. [cited 23 Oct 2020]. Available: https://www.medrxiv.org/content/10.1101/2020.09.30.20204644v1

8. Dorigatti I, Okell L, Cori A, Imai N, Baguelin M, Bhatia S, et al. Report 4: Severity of 2019-novel coronavirus (nCoV). Imperial College London; 2020 Feb. Report No.: 4. doi:10.25561/77154

9. Onder G, Rezza G, Brusaferro S. Case-Fatality Rate and Characteristics of Patients Dying in Relation to COVID-19 in Italy. JAMA. 2020 [cited 23 Oct 2020]. doi:10.1001/jama.2020.4683

10. Russell TW, Hellewell J, Jarvis CI, Zandvoort K van, Abbott S, Ratnayake R, et al. Estimating the infection and case fatality ratio for coronavirus disease (COVID-19) using age-adjusted data from the outbreak on the Diamond Princess cruise ship, February 2020. Eurosurveillance. 2020;25: 2000256. doi:10.2807/1560-7917.ES.2020.25.12.2000256

11. Wu JT, Leung K, Bushman M, Kishore N, Niehus R, de Salazar PM, et al. Estimating clinical severity of COVID-19 from the transmission dynamics in Wuhan, China. Nat Med. 2020; 1–5. doi:10.1038/s41591-020-0822-7

12. Unwin H, Mishra S, Bradley V, Gandy A, Vollmer M, Mellan T, et al. Report 23: State-level tracking of COVID-19 in the United States. Imperial College London; 2020 May. doi:10.25561/79231

13. Flaxman S, Mishra S, Gandy A, Unwin HJT, Mellan TA, Coupland H, et al. Estimating the effects of non-pharmaceutical interventions on COVID-19 in Europe. Nature. 2020;584: 257–261. doi:10.1038/s41586-020-2405-7

14. Badr HS, Du H, Marshall M, Dong E, Squire MM, Gardner LM. Association between mobility patterns and COVID-19 transmission in the USA: a mathematical modelling study. Lancet Infect Dis. 2020;20: 1247–1254. doi:10.1016/S1473-3099(20)30553-3

15. Tian H, Liu Y, Li Y, Wu C-H, Chen B, Kraemer MUG, et al. An investigation of transmission control measures during the first 50 days of the COVID-19 epidemic in China. Science. 2020;368: 638–642. doi:10.1126/science.abb6105

16. Kraemer MUG, Yang C-H, Gutierrez B, Wu C-H, Klein B, Pigott DM, et al. The effect of human mobility and control measures on the COVID-19 epidemic in China. Science. 2020;368: 493–497. doi:10.1126/science.abb4218

17. Kishore N, Kiang MV, Engø-Monsen K, Vembar N, Schroeder A, Balsari S, et al. Measuring mobility to monitor travel and physical distancing interventions: a common framework for mobile phone data analysis. Lancet Digit Health. 2020;2: e622–e628. doi:10.1016/S2589-7500(20)30193-X

18. Buckee CO, Balsari S, Chan J, Crosas M, Dominici F, Gasser U, et al. Aggregated mobility data could help fight COVID-19. Science. 2020;368: 145–146. doi:10.1126/science.abb8021

19. COVID-19 Mobility Data Network. In: COVID-19 Mobility Data Network [Internet]. [cited 28 Oct 2020]. Available: https://www.covid19mobility.org/

20. Maas P. Facebook Disaster Maps: Aggregate Insights for Crisis Response & Recovery. Proceedings of the 25th ACM SIGKDD International Conference on Knowledge Discovery & Data Mining. New York, NY, USA: Association for Computing Machinery; 2019. p. 3173. doi:10.1145/3292500.3340412

21. Russell TW, Golding N, Hellewell J, Abbott S, Wright L, Pearson CAB, et al. Reconstructing the early global dynamics of under-ascertained COVID-19 cases and infections. medRxiv. 2020; 2020.07.07.20148460. doi:10.1101/2020.07.07.20148460

22. Chitwood MH, Russi M, Gunasekera K, Havumaki J, Pitzer VE, Warren JL, et al. Bayesian nowcasting with adjustment for delayed and incomplete reporting to estimate COVID-19 infections in the United States. medRxiv. 2020; 2020.06.17.20133983. doi:10.1101/2020.06.17.20133983

23. Lewnard JA, Liu VX, Jackson ML, Schmidt MA, Jewell BL, Flores JP, et al. Incidence, clinical outcomes, and transmission dynamics of severe coronavirus disease 2019 in California and Washington: prospective cohort study. BMJ. 2020;369: m1923. doi:10.1136/bmj.m1923

24. Davies NG, Klepac P, Liu Y, Prem K, Jit M, Eggo RM. Age-dependent effects in the transmission and control of COVID-19 epidemics. Nat Med. 2020; 1–7. doi:10.1038/s41591-020-0962-9

25. Pham QT, Rabaa MA, Duong HL, Dang QT, Tran DQ, Quach H-L, et al. The first 100 days of SARS-CoV-2 control in Vietnam. Clin Infect Dis. [cited 11 Nov 2020]. doi:10.1093/cid/ciaa1130

26. Van Vinh Chau N, Lam VT, Dung NT, Yen LM, Minh NNQ, Hung LM, et al. The Natural History and Transmission Potential of Asymptomatic Severe Acute Respiratory Syndrome Coronavirus 2 Infection. Clin Infect Dis. [cited 11 Nov 2020]. doi:10.1093/cid/ciaa711

27. Kimball A. Asymptomatic and Presymptomatic SARS-CoV-2 Infections in Residents of a Long-Term Care Skilled Nursing Facility — King County, Washington, March 2020. MMWR Morb Mortal Wkly Rep. 2020;69. doi:10.15585/mmwr.mm6913e1

28. Lytras T, Dellis G, Flountzi A, Hatzianastasiou S, Nikolopoulou G, Tsekou K, et al. High prevalence of SARS-CoV-2 infection in repatriation flights to Greece from three European countries. J Travel Med. 2020;27. doi:10.1093/jtm/taaa054

29. RI Department of Health COVID-19 Response (TESTING DATA). [cited 23 Oct 2020]. Available: https://ri-department-of-health-covid-19-response-demogr-a3f82-rihealth.hub.arcgis.com/

30. Nesbitt DJ, Jin D, Hogan JW, Chan PA, Simon MJ, Vargas M, et al. Low Seroprevalence of SARS-CoV-2 in Rhode Island Blood Donors Determined using Multiple Serological Assay Formats. medRxiv. 2020; 2020.07.20.20157743. doi:10.1101/2020.07.20.20157743

31. Havers FP, Reed C, Lim T, Montgomery JM, Klena JD, Hall AJ, et al. Seroprevalence of Antibodies to SARS-CoV-2 in 10 Sites in the United States, March 23-May 12, 2020. JAMA Intern Med. 2020 [cited 23 Oct 2020]. doi:10.1001/jamainternmed.2020.4130

32. Anand S, Montez-Rath M, Han J, Bozeman J, Kerschmann R, Beyer P, et al. Prevalence of SARS-CoV-2 antibodies in a large nationwide sample of patients on dialysis in the USA: a cross-sectional study. The Lancet. 2020;396: 1335–1344. doi:10.1016/S0140-6736(20)32009-2

33. Herrera-Esposito D, Campos G de los. Age-specific rate of severe and critical SARS-CoV-2 infections estimated with multi-country seroprevalence studies. 2021 Jul p. 2021.07.29.21261282. doi:10.1101/2021.07.29.21261282

34. Levin AT, Hanage WP, Owusu-Boaitey N, Cochran KB, Walsh SP, Meyerowitz-Katz G. Assessing the age specificity of infection fatality rates for COVID-19: systematic review, meta-analysis, and public policy implications. Eur J Epidemiol. 2020;35: 1123–1138. doi:10.1007/s10654-020-00698-1

35. Lapidus N, Paireau J, Levy-Bruhl D, de Lamballerie X, Severi G, Touvier M, et al. Do not neglect SARS-CoV-2 hospitalization and fatality risks in the middle-aged adult population. Infect Dis Now. 2021;51: 380–382. doi:10.1016/j.idnow.2020.12.007

36. O'Driscoll M, Ribeiro Dos Santos G, Wang L, Cummings DAT, Azman AS, Paireau J, et al. Age-specific mortality and immunity patterns of SARS-CoV-2. Nature. 2021;590: 140–145. doi:10.1038/s41586-020-2918-0

37. Brazeau NF. Report 34 - COVID-19 Infection Fatality Ratio Estimates from Seroprevalence. In: Imperial College London [Internet]. [cited 11 Aug 2021]. Available: http://www.imperial.ac.uk/medicine/departments/school-public-health/infectious-disease-epidemiology/mrc-global-infectious-disease-analysis/covid-19/report-34-ifr/

38. Yang W, Kandula S, Huynh M, Greene SK, Van Wye G, Li W, et al. Estimating the infection-fatality risk of SARS-CoV-2 in New York City during the spring 2020 pandemic wave: a model-based analysis. Lancet Infect Dis. 2021;21: 203–212. doi:10.1016/S1473-3099(20)30769-6

39. TheOpenSafelyCollaborative, Williamson E, Walker AJ, Bhaskaran KJ, Bacon S, Bates C, et al. OpenSAFELY: factors associated with COVID-19-related hospital death in the linked electronic health records of 17 million adult NHS patients. medRxiv. 2020; 2020.05.06.20092999. doi:10.1101/2020.05.06.20092999

40. Gupta S, Hayek SS, Wang W, Chan L, Mathews KS, Melamed ML, et al. Factors Associated With Death in Critically Ill Patients With Coronavirus Disease 2019 in the US. JAMA Intern Med. 2020;180: 1436. doi:10.1001/jamainternmed.2020.3596

41. Dorélien AM, Simon A, Hagge S, Call KT, Enns E, Kulasingam S. Minnesota Social Contacts and Mixing Patterns Survey with Implications for Modelling of Infectious Disease Transmission and Control. Surv Pract. 2020;13: 13669. doi:10.29115/SP-2020-0007

42. Feehan D, Mahmud A. Quantifying population contact patterns in the United States during the COVID-19 pandemic. medRxiv. 2020; 2020.04.13.20064014. doi:10.1101/2020.04.13.20064014

43. Coletti P, Wambua J, Gimma A, Willem L, Vercruysse S, Vanhoutte B, et al. CoMix: comparing mixing patterns in the Belgian population during and after lockdown. medRxiv. 2020; 2020.08.06.20169763. doi:10.1101/2020.08.06.20169763

44. Jarvis CI, Van Zandvoort K, Gimma A, Prem K, Auzenbergs M, O'Reilly K, et al. Quantifying the impact of physical distance measures on the transmission of COVID-19 in the UK. BMC Med. 2020;18: 124. doi:10.1186/s12916-020-01597-8

45. Zhang J, Litvinova M, Liang Y, Wang Y, Wang W, Zhao S, et al. Changes in contact patterns shape the dynamics of the COVID-19 outbreak in China. Science. 2020;368: 1481–1486. doi:10.1126/science.abb8001

46. Coletti P, Wambua J, Gimma A, Willem L, Vercruysse S, Vanhoutte B, et al. CoMix: comparing mixing patterns in the Belgian population during and after lockdown. Sci Rep. 2020;10: 21885. doi:10.1038/s41598-020-78540-7

47. Tran TN-A, Wikle NB, Albert E, Inam H, Strong E, Brinda K, et al. Optimal SARS-CoV-2 vaccine allocation using real-time attack-rate estimates in Rhode Island and Massachusetts. BMC Med. 2021;19: 162. doi:10.1186/s12916-021-02038-w

48. Sartini C, Tresoldi M, Scarpellini P, Tettamanti A, Carcò F, Landoni G, et al. Respiratory Parameters in Patients With COVID-19 After Using Noninvasive Ventilation in the Prone Position Outside the Intensive Care Unit. JAMA. 2020;323: 2338. doi:10.1001/jama.2020.7861

49. Elharrar X, Trigui Y, Dols A-M, Touchon F, Martinez S, Prud'homme E, et al. Use of Prone Positioning in Nonintubated Patients With COVID-19 and Hypoxemic Acute Respiratory Failure. JAMA. 2020;323: 2336. doi:10.1001/jama.2020.8255

50. TheRECOVERYCollaborativeGroup. Dexamethasone in Hospitalized Patients with Covid-19 — Preliminary Report. N Engl J Med. 2020 [cited 14 Nov 2020]. doi:10.1056/NEJMoa2021436

51. Fadel R, Morrison AR, Vahia A, Smith ZR, Chaudhry Z, Bhargava P, et al. Early Short-Course Corticosteroids in Hospitalized Patients With COVID-19. Clin Infect Dis. [cited 14 Nov 2020]. doi:10.1093/cid/ciaa601

52. Horwitz LI, Jones SA. Trends in COVID-19 Risk-Adjusted Mortality Rates. J Hosp Med. 2020 [cited 30 Oct 2020]. doi:10.12788/jhm.3552

53. Characteristics and Outcomes of COVID-19 Patients During Initial Peak and Resurgence in the Houston Metropolitan Area | Critical Care Medicine | JAMA | JAMA Network. [cited 30 Oct 2020]. Available: https://jamanetwork.com/journals/jama/fullarticle/2769610

54. Dennis J, McGovern A, Vollmer S, Mateen BA. Improving COVID-19 critical care mortality over time in England: A national cohort study, March to June 2020. medRxiv. 2020; 2020.07.30.20165134. doi:10.1101/2020.07.30.20165134

55. Salje H, Tran Kiem C, Lefrancq N, Courtejoie N, Bosetti P, Paireau J, et al. Estimating the burden of SARS-CoV-2 in France. Science. 2020;369: 208–211. doi:10.1126/science.abc3517

56. Petrilli CM, Jones SA, Yang J, Rajagopalan H, O'Donnell L, Chernyak Y, et al. Factors associated with hospital admission and critical illness among 5279 people with coronavirus disease 2019 in New York City: prospective cohort study. BMJ. 2020;369: m1966. doi:10.1136/bmj.m1966

57. Weinberger DM, Chen J, Cohen T, Crawford FW, Mostashari F, Olson D, et al. Estimation of Excess Deaths Associated With the COVID-19 Pandemic in the United States, March to May 2020. JAMA Intern Med. 2020;180: 1336–1344. doi:10.1001/jamainternmed.2020.3391

58. Larremore DB, Fosdick BK, Bubar KM, Zhang S, Kissler SM, Metcalf CJE, et al. Estimating SARS-CoV-2 seroprevalence and epidemiological parameters with uncertainty from serological surveys. medRxiv. 2020; 2020.04.15.20067066. doi:10.1101/2020.04.15.20067066

59. Ainslie K, Walters C, Fu H, Bhatia S, Wang H, Baguelin M, et al. Report 11: Evidence of initial success for China exiting COVID-19 social distancing policy after achieving containment. Imperial College London; 2020 Mar. doi:10.25561/77646

60. Unwin HJT, Mishra S, Bradley VC, Gandy A, Mellan TA, Coupland H, et al. State-level tracking of COVID-19 in the United States. Nat Commun. 2020;11: 6189. doi:10.1038/s41467-020-19652-6

61. Monod M, Blenkinsop A, Xi X, Hebert D, Bershan S, Tietze S, et al. Age groups that sustain resurging COVID-19 epidemics in the United States. Science. 2021;371. doi:10.1126/science.abe8372

62. Penn State CIDD COVID Modeling Team. Attack Rate Summary, 11-20-2020. Available: https://mol.ax/covid/attack-rate-11-20/

63. CDC. Nationwide Commercial Laboratory Seroprevalence Survey. [cited 12 Aug 2021]. Available: https://covid.cdc.gov/covid-data-tracker/#national-lab

64. CDC. Nationwide Blood Donor Seroprevalence Survey. [cited 12 Aug 2021]. Available: https://covid.cdc.gov/covid-data-tracker/#nationwide-blood-donor-seroprevalence

65. Bajema KL, Wiegand RE, Cuffe K, Patel SV, Iachan R, Lim T, et al. Estimated SARS-CoV-2 Seroprevalence in the US as of September 2020. JAMA Intern Med. 2021;181: 450–460. doi:10.1001/jamainternmed.2020.7976

66. Boni MF, Mølbak K, Krogfelt KA. Inferring the time of infection from serological data. Handbook of Infectious Disease Data Analysis. Boca Raton, FL: Taylor & Francis, CRC Press; 2020. pp. 287–303.

67. Levin AT, Hanage WP, Owusu-Boaitey N, Cochran KB, Walsh SP, Meyerowitz-Katz G. Assessing the Age Specificity of Infection Fatality Rates for COVID-19: Systematic Review, Meta-Analysis, and Public Policy Implications. medRxiv. 2020; 2020.07.23.20160895. doi:10.1101/2020.07.23.20160895

68. Verity R, Okell LC, Dorigatti I, Winskill P, Whittaker C, Imai N, et al. Estimates of the severity of coronavirus disease 2019: a model-based analysis. Lancet Infect Dis. 2020;20: 669–677. doi:10.1016/S1473-3099(20)30243-7

69. CDCMMWR. Severe Outcomes Among Patients with Coronavirus Disease 2019 (COVID-19) — United States, February 12–March 16, 2020. MMWR Morb Mortal Wkly Rep. 2020;69. doi:10.15585/mmwr.mm6912e2

70. Ahammed T, Anjum A, Rahman MM, Haider N, Kock R, Uddin MJ. Estimation of novel coronavirus (covid-19) reproduction number and case fatality rate: a systematic review and meta-analysis. medRxiv. 2020; 2020.09.30.20204644. doi:10.1101/2020.09.30.20204644

71. Mandavilli A, Stolberg SG. A Viral Theory Cited by Health Officials Draws Fire From Scientists. The New York Times. 23 Oct 2020. Available: https://www.nytimes.com/2020/10/19/health/coronavirus-great-barrington.html. Accessed 1 Nov 2020.

72. Wikle N, Tran TN-A, Gentilesco B, Leighow SM, Albert J, Strong ER, et al. SARS-CoV-2 epidemic after social and economic reopening in three US states reveals shifts in age structure and clinical characteristics. medRxiv. 2020; 2020.11.17.20232918v1. doi:10.1101/2020.11.17.20232918

73. Covid-19 in the US: We're not getting full value from our data. In: The BMJ [Internet]. 6 Jul 2020 [cited 30 Oct 2020]. Available: https://blogs.bmj.com/bmj/2020/07/06/covid-19-in-the-us-were-not-getting-full-value-from-our-data/

74. Penn State CIDD COVID Modeling Team. Massachusetts June 30 Preliminary Analysis. Available: https://mol.ax/covid/massachusetts-06-30/

75. Social Distancing Metrics. In: SafeGraph [Internet]. [cited 14 Nov 2020]. Available: https://docs.safegraph.com/docs/social-distancing-metrics

76. Shelter in Place Index: The Impact of Coronavirus on Human Movement. In: SafeGraph [Internet]. [cited 14 Nov 2020]. Available: https://safegraph.com/data-examples/covid19-shelter-in-place/

77. Measuring and Correcting Sampling Bias in Safegraph Patterns for More Accurate Demographic Analysis. [cited 14 Nov 2020]. Available: https://www.safegraph.com/blog/measuring-and-correcting-sampling-bias-for-accurate-demographic-analysis

78. Ferguson N, Laydon D, Nedjati Gilani G, Imai N, Ainslie K, Baguelin M, et al. Report 9: Impact of non-pharmaceutical interventions (NPIs) to reduce COVID19 mortality and healthcare demand. Imperial College London; 2020 Mar. doi:10.25561/77482

79. Davies NG, Kucharski AJ, Eggo RM, Gimma A, Edmunds WJ, Jombart T, et al. Effects of non-pharmaceutical interventions on COVID-19 cases, deaths, and demand for hospital services in the UK: a modelling study. Lancet Public Health. 2020;5: e375–e385. doi:10.1016/S2468-2667(20)30133-X

80. Shaby B, Wells MT. Exploring an adaptive metropolis algorithm. 2010.

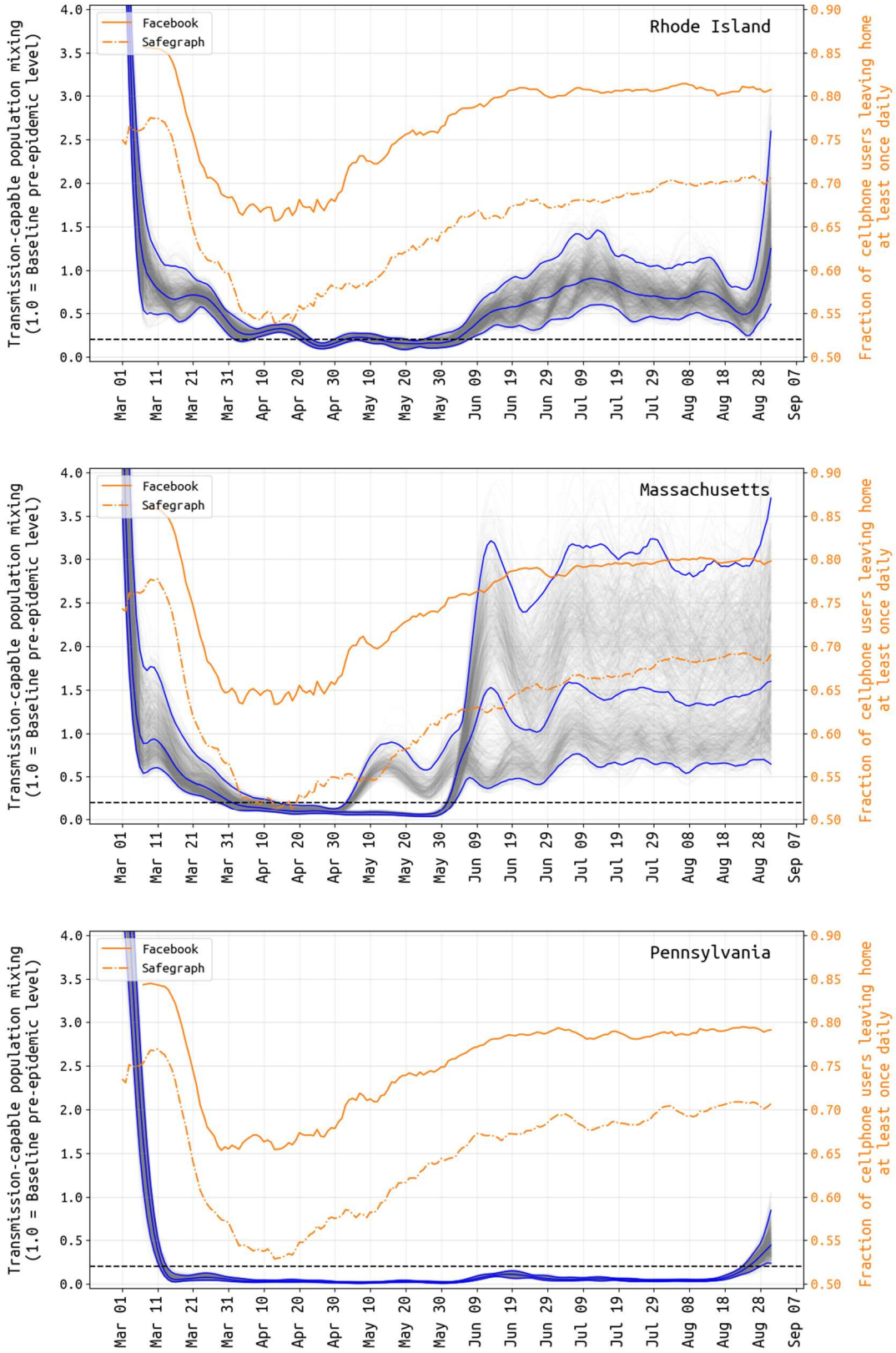

Figure 1. Transmission-capable population-level mixing β_t (in gray and blue) and mobility changes (yellow) from March 1 to August 31. The average population mixing for March 5-15 is set to 1.0 as the pre-epidemic level of transmission-capable mixing, and all other values are reported relative to this. Gray lines show 1000 sampled posterior β-trajectories with the blue lines showing the median and 95% credible intervals. Note that there is substantial uncertainty in these estimates during the first weeks of March, as case numbers were low and reporting may not have been catching a large proportion of true cases at this time. Yellow lines show the fraction of Facebook and SafeGraph users that left home at least once per day. The correlation between population-movement (yellow) and transmission-capable population movement (gray+blue) begins to disappear in early May in RI and PA (and with less certainty, in MA).

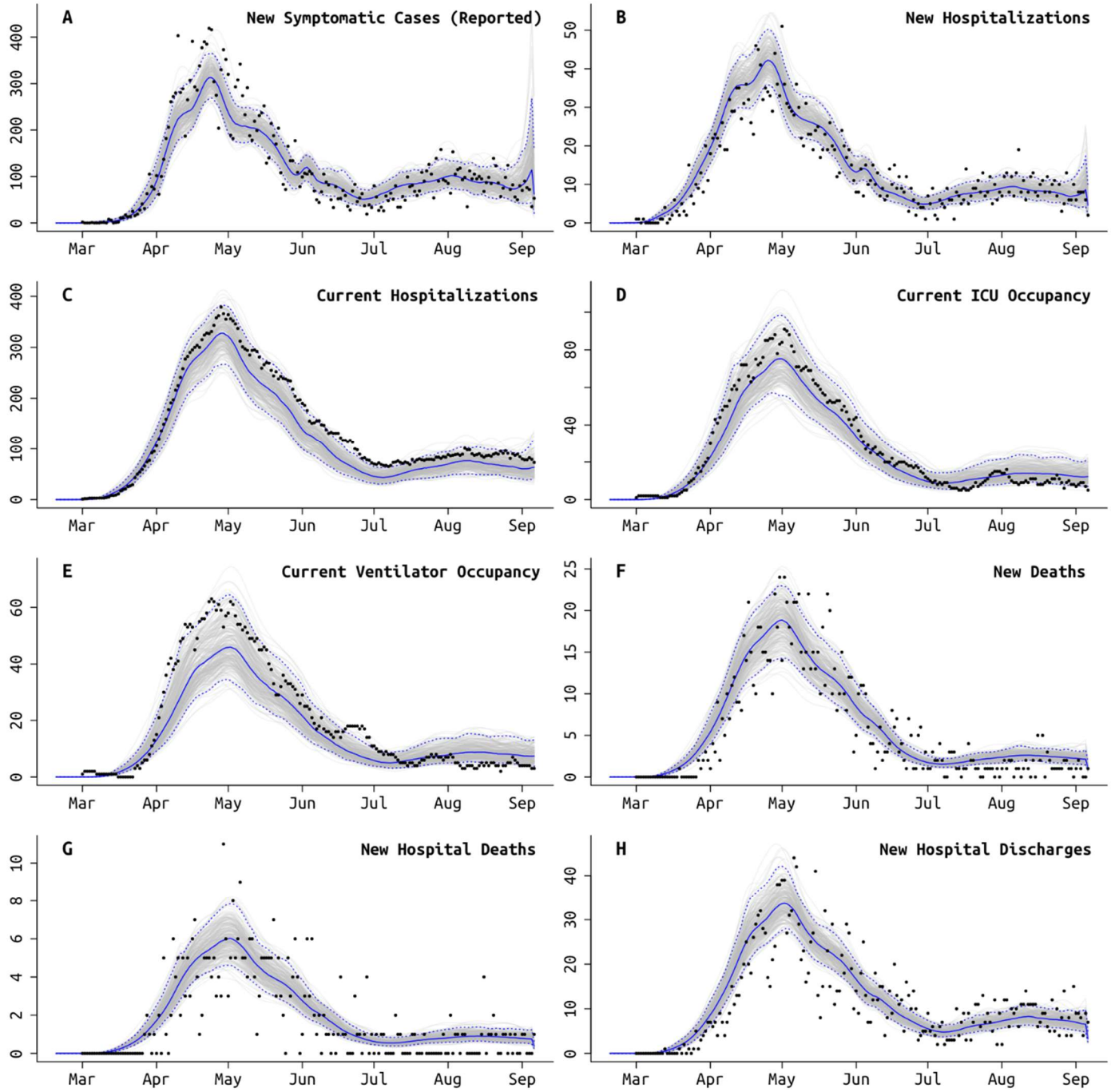

Figure 2: Model fit to Rhode Island daily data, using the best fit model which accounts for different age-based contact rates after the lockdown and a different rate of ICU admissions starting in early June (Table 2). Gray lines show 250 sampled trajectories from the posterior, and blue lines are the median trajectories. Black circles are data points that show the daily (**A**) newly reported symptomatic cases, (**B**) new hospitalizations, (**C**) current number of patients hospitalized, (**D**) current number of patients in critical care, (**E**) current number of patients undergoing mechanical ventilation, (**F**) new deaths reported, (**G**) new hospital deaths reported, i.e. excluding deaths that occurred at home or at long-term care facilities, and (**H**) number of hospital discharges. Model fits for MA and PA are shown in Figures S13 and S14.

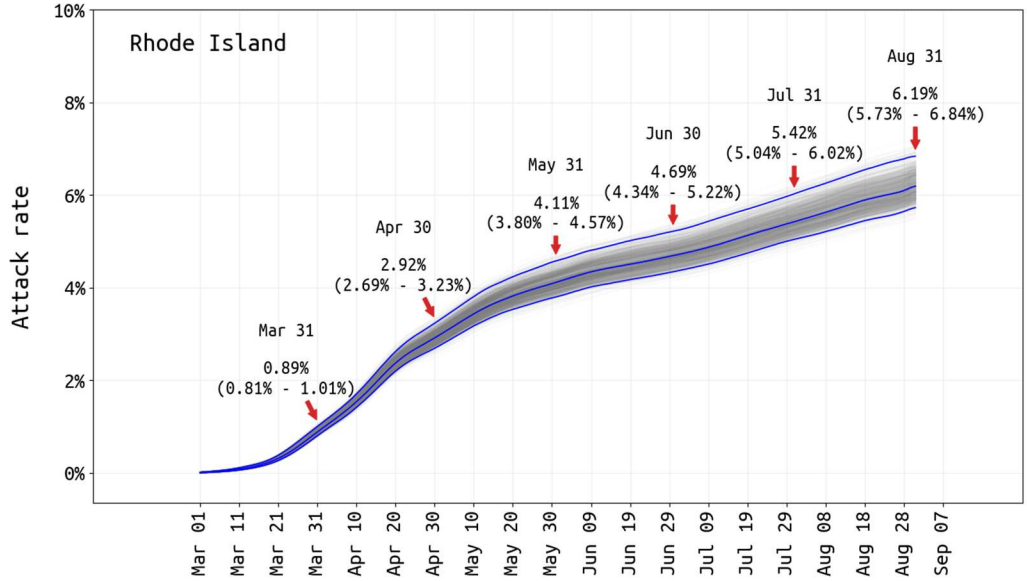
Rhode Island
Attack rate
10%
8%
6%
4%
2%
0%
Mar 31
0.89%
(0.81% - 1.01%)
Apr 30
2.92%
(2.69% - 3.23%)
May 31
4.11%
(3.80% - 4.57%)
Jun 30
4.69%
(4.34% - 5.22%)
Jul 31
5.42%
(5.04% - 6.02%)
Aug 31
6.19%
(5.73% - 6.84%)
Mar 01
Mar 11
Mar 21
Mar 31
Apr 10
Apr 20
Apr 30
May 10
May 20
May 30
Jun 09
Jun 19
Jun 29
Jul 09
Jul 19
Jul 29
Aug 08
Aug 18
Aug 28
Sep 07

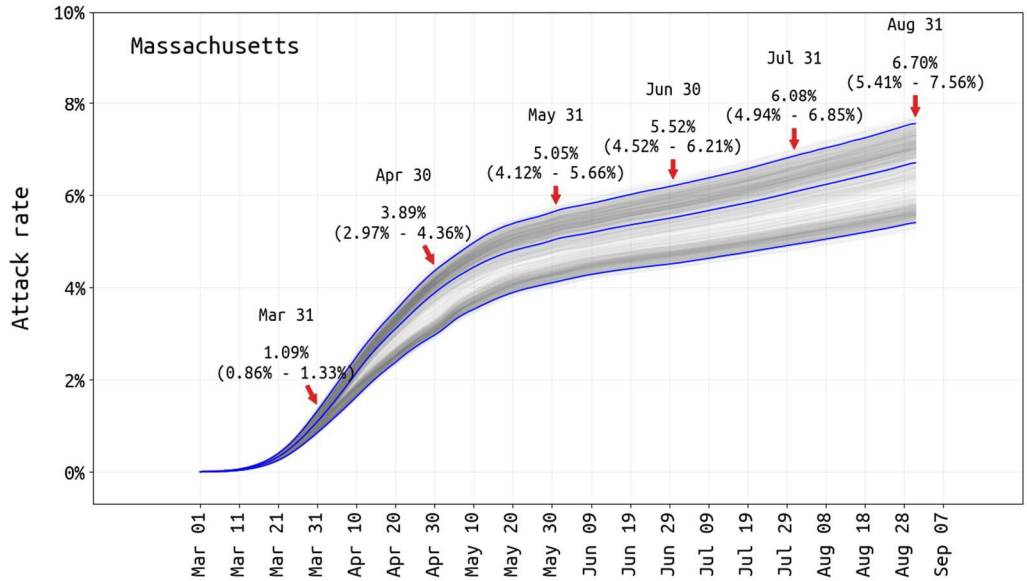
Massachusetts
Attack rate
10%
8%
6%
4%
2%
0%
Mar 31
1.09%
(0.86% - 1.33%)
Apr 30
3.89%
(2.97% - 4.36%)
May 31
5.05%
(4.12% - 5.66%)
Jun 30
5.52%
(4.52% - 6.21%)
Jul 31
6.08%
(4.94% - 6.85%)
Aug 31
6.70%
(5.41% - 7.56%)
Mar 01
Mar 11
Mar 21
Mar 31
Apr 10
Apr 20
Apr 30
May 10
May 20
May 30
Jun 09
Jun 19
Jun 29
Jul 09
Jul 19
Jul 29
Aug 08
Aug 18
Aug 28
Sep 07

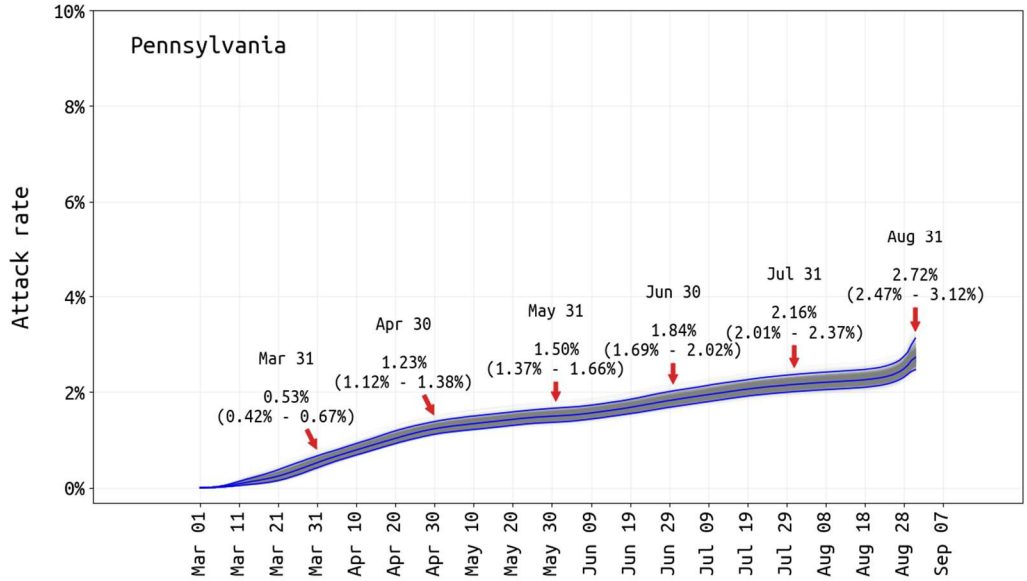
Pennsylvania
Attack rate
10%
8%
6%
4%
2%
0%
Mar 31
0.53%
(0.42% - 0.67%)
Apr 30
1.23%
(1.12% - 1.38%)
May 31
1.50%
(1.37% - 1.66%)
Jun 30
1.84%
(1.69% - 2.02%)
Jul 31
2.16%
(2.01% - 2.37%)
Aug 31
2.72%
(2.47% - 3.12%)
Mar 01
Mar 11
Mar 21
Mar 31
Apr 10
Apr 20
Apr 30
May 10
May 20
May 30
Jun 09
Jun 19
Jun 29
Jul 09
Jul 19
Jul 29
Aug 08
Aug 18
Aug 28
Sep 07

Figure 3. Posterior distribution of total attack rate through August 31 2020. Total infection attack rate includes all reported symptomatic cases, estimated unreported symptomatic infections, and estimated asymptomatic infections. Cumulative attack-rate estimates and 95% credible intervals are shown for the end of every month.

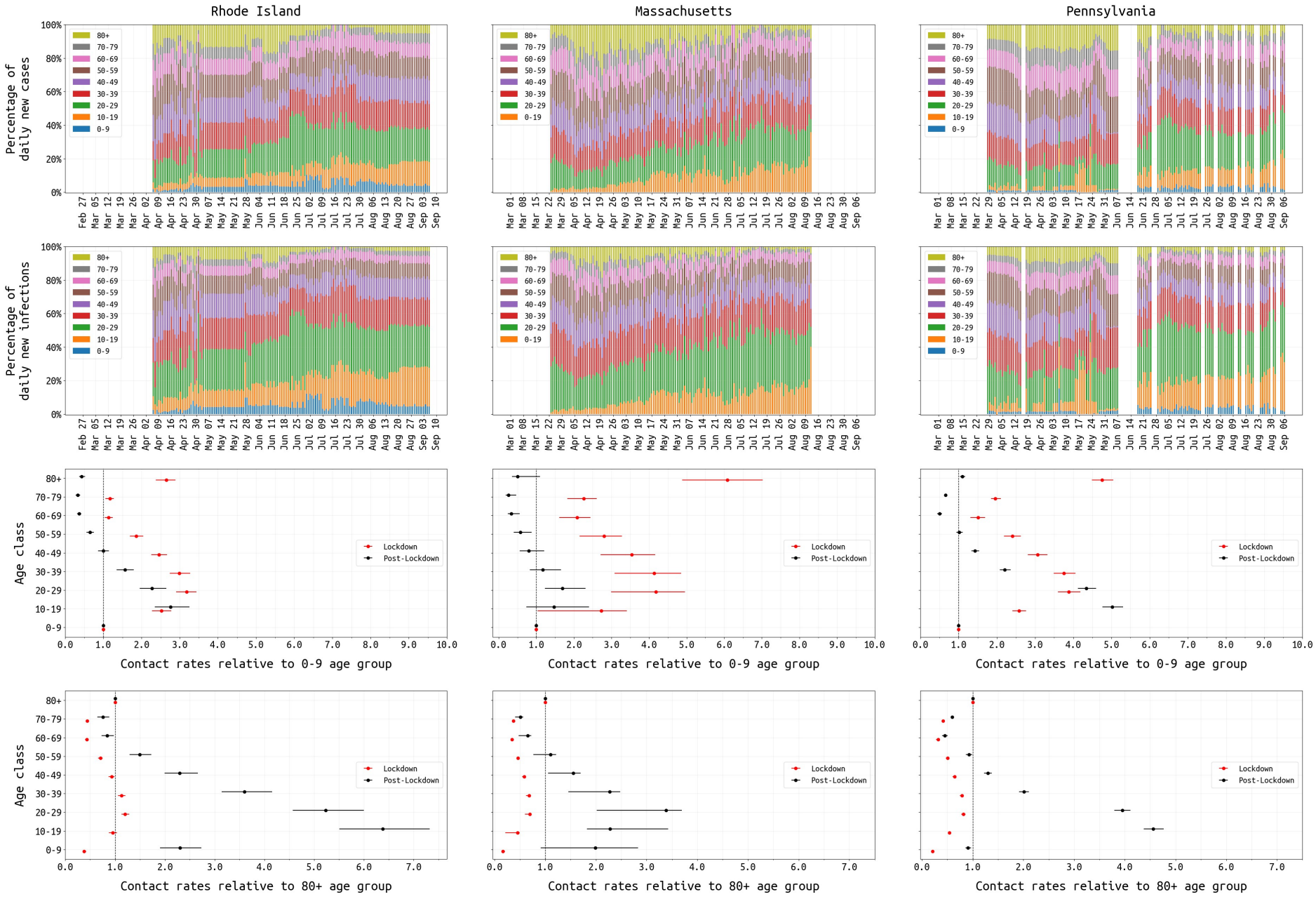
Rhode Island
Massachusetts
Pennsylvania
Percentage of daily new cases
Percentage of daily new infections
80+
70-79
60-69
50-59
40-49
30-39
20-29
10-19
0-9
Age class
Lockdown
Post-Lockdown
Contact rates relative to 0-9 age group
Contact rates relative to 80+ age group

Figure 4. Changing age-structure of COVID-19 epidemics in RI, MA, and PA. Top rows shows the age structure of reported cases (*first row*) and estimated infections (*second row*) from March 1 to August 31. RI and PA report age data periodically; missing values have been linearly interpolated in RI. *Third row* shows the inferred age-specific contact rates (median and 95% credible intervals) for both the lockdown (red) and post-lockdown period (black), where the reference group is the 0-9 age group. *Fourth row* shows these same inferred contact rates with the ≥80 age group as the reference.

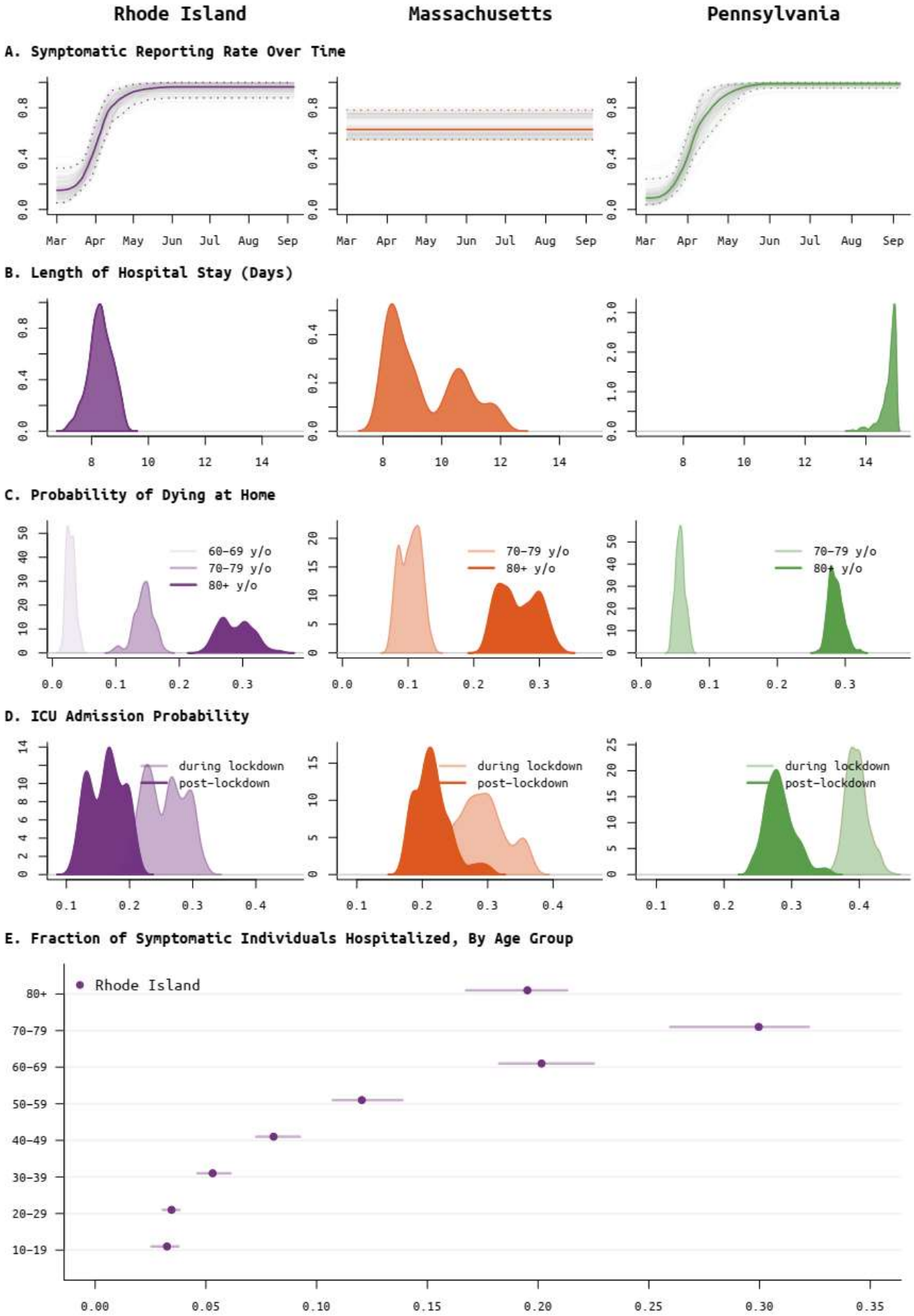
Rhode Island
Massachusetts
Pennsylvania
A. Symptomatic Reporting Rate Over Time
Mar Apr May Jun Jul Aug Sep
B. Length of Hospital Stay (Days)
C. Probability of Dying at Home
60–69 y/o
70–79 y/o
80+ y/o
D. ICU Admission Probability
during lockdown
post-lockdown
E. Fraction of Symptomatic Individuals Hospitalized, By Age Group
Rhode Island
80+
70–79
60–69
50–59
40–49
30–39
20–29
10–19

Figure 5. Posterior distributions of reporting rate (panel **A**) and clinical parameters (panels **B** to **E**) for Rhode Island (purple, left column), Massachusetts (orange, middle column), and Pennsylvania (green, right column). (**A**) Reporting parameter ρ, i.e. the fraction of symptomatic SARS-CoV-2 cases that are reported to the health system, plotted as a function of time. In Rhode Island, it was known that in March testing was not available and cases could not be confirmed; therefore a spline function was fit for ρ. This same function provided a better fit for Pennsylvania data, but not for Massachusetts data. (**B**) Median length of medical-floor hospital stay was 8.3 days in RI, 8.9 days in MA, and 14.9 days in PA. (**C**) Probabilities of dying at home for the 60-69, 70-79, and 80+ age groups; 60-69 age group was included only for RI as data were insufficient in PA and MA. These are largely reflective of the epidemics passing through nursing home populations where individuals are not counted as hospitalized if they remain in care at their congregate care facility in a severe or advanced clinical state. These probabilities are important when accounting for hospital bed capacity in forecasts. (**D**) Age-adjusted ICU admission probability during the lockdown period in spring 2020 (lighter color) and after the lockdown (darker color). (**E**) Probability of hospitalization (median and 95% CIs) for symptomatic SARS-CoV-2 infections, by age group; estimates only available for RI.

Tables

Table 1. Infection fatality rate (IFR), symptomatic case fatality rate (sCFR), and hospitalization fatality rate (HFR) for the March-June COVID-19 epidemics in RI, MA, and PA. Numbers of deaths observed in the <20 age groups were too low to generate meaningful estimates. CI: credible interval.

Age Range	State	IFR (95% CI)	sCFR (95% CI)	HFR (95% CI)
20-29	RI	<5 deaths	<5 deaths	<5 deaths
	MA	0.03% (0.03% - 0.04%)	0.12% (0.10% – 0.15%)	3.3% (2.7% – 4.1%)
	PA	0.04% (0.04% - 0.04%)	0.16% (0.14% - 0.17%)	4.5% (4.2% - 4.9%)
30-39	RI	0.05% (0.04% – 0.07%)	0.16% (0.13% – 0.21%)	3.2% (2.5% – 3.8%)
	MA	0.06% (0.05% – 0.08%)	0.19% (0.16% – 0.24%)	3.6% (2.9% - 4.4%)
	PA	0.09% (0.08% - 0.10%)	0.26% (0.23% - 0.29%)	4.8% (4.4% - 5.2%)
40-49	RI	0.31% (0.22% – 0.38%)	0.78% (0.55% – 0.96%)	9.6% (7.2% – 12.2%)
	MA	0.33% (0.26% – 0.44%)	0.83% (0.65% - 1.11%)	10.2% (7.8% - 12.8%)
	PA	0.58% (0.52% - 0.65%)	1.44% (1.31% - 1.63%)	17.9% (16.0% - 20.2%)
50-59	RI	0.60% (0.44% – 0.73%)	1.24% (0.90% – 1.49%)	10.2% (7.6% – 12.8%)
	MA	0.66% (0.49% - 0.85%)	1.34% (1.01% - 1.74%)	10.8% (8.2% - 13.5%)
	PA	1.16% (1.06% - 1.30%)	2.37% (2.16% - 2.64%)	18.8% (16.9% - 21.3%)
60-69	RI	3.2% (2.5% – 4.1%)	5.1% (3.9% – 6.6%)	14.0% (10.5% – 17.7%)
	MA	3.2% (2.4% - 3.9%)	5.0% (3.9% - 6.2%)	14.8% (11.3% - 18.6%)
	PA	4.6% (4.2% - 5.0%)	7.3% (6.6% - 7.9%)	26.0% (23.2% - 29.4%)
70-79	RI	12.1% (9.2% – 13.8%)	17.5% (13.3% – 20.0%)	25.4% (20.4% – 29.9%)
	MA	10.9% (8.9% - 13.1%)	15.8% (12.9% - 19.0%)	28.2% (23.6% - 34.5%)
	PA	12.6% (12.0% - 13.4%)	18.2% (17.5% - 19.4%)	37.0% (34.6% - 40.2%)
≥80	RI	19.9% (17.1% – 23.5%)	28.9% (24.8% – 34.0%)	29.7% (24.4% – 34.5%)
	MA	19.2% (16.3% - 22.9%)	27.8% (23.7% - 33.2%)	32.8% (27.8% - 39.6%)
	PA	21.7% (20.6% - 23.5%)	31.5% (29.8% - 34.1%)	42.4% (39.7% - 45.8%)

Table 2. Deviance Information Criterion (DIC) values for different models. Minimum DIC values shown in boldface.

	No change in age-profile of contact rates post lockdown. No change in ICU admission rate from March to August.	Different age-profile of population contact rates post lockdown (approx May 2020). No change in ICU admission rate from March to August	No change in age-profile of contact rates post lockdown. Allows for change in ICU admission rate from March to August.	Different age-profile of population contact rates post lockdown (approx May 2020). Allows for change in ICU admission rate from March to August.
RI	12064	11059	11960	**11004**
MA	26123	18710	26328	**17603**
PA	18858	10626	18851	**10599**